

Available online at www.sciencedirect.com

ScienceDirect

Procedia Chemistry 19 (2016) 949 – 954

Procedia
Chemistry

5th International Conference on Recent Advances in Materials, Minerals and Environment (RAMM) & 2nd International Postgraduate Conference on Materials, Mineral and Polymer (MAMIP), 4-6 August 2015

Comparative Study on the Effect of Zr^{4+} and Ca^{2+} Doping on the Properties of NiO

J.J. Mohamed ^{a*}, S.A.S. Salim ^b and Z.A. Ahmad ^b

^aAdvance Materials Research Cluster, Faculty of Earth Science, Universiti Malaysia Kelantan, Locked Bag 36, Pengkalan Chepa, 16100 Kota Bharu, Kelantan.

^bStructural Materials Niche Area, School of Materials and Mineral Resources Engineering, Universiti Sains Malaysia, Engineering Campus, Seri Ampangan, 14300 Nibong Tebal, Penang, Malaysia.

Abstract

The comparative study was made on the effect of Zirconium ions (Zr^{4+}) and Calcium ions (Ca^{2+}) dopant on NiO properties. The electroceramic of $\text{Ni}_{(1-x)}\text{Zr}_x\text{O}$ and $\text{Ni}_{(1-x)}\text{Ca}_x\text{O}$ was prepared by using solid state reaction method. The different amount of Zr^{4+} was studied. XRD analysis on sintered sample showed the single phase formation of $\text{Ni}_{(1-x)}\text{Zr}_x\text{O}$ and $\text{Ni}_{(1-x)}\text{Ca}_x\text{O}$. The dielectric behavior of $\text{Ni}_{(1-x)}\text{Zr}_x\text{O}$ with $x = 0.02$ mole % Zr^{4+} exhibited highest dielectric constant (700) with moderate dielectric loss (0.16). Meanwhile, the dielectric behavior of $\text{Ni}_{(1-x)}\text{Ca}_x\text{O}$ samples show that the sample doped with $x = 0.01$ mole % Ca^{2+} obtained the lowest dielectric loss (0.05) but moderate in dielectric constant (123), measured at 1 MHz.

© 2016 The Authors. Published by Elsevier B.V. This is an open access article under the CC BY-NC-ND license

(<http://creativecommons.org/licenses/by-nc-nd/4.0/>).

Peer-review under responsibility of School of Materials and Mineral Resources Engineering, Universiti Sains Malaysia

Keywords: Zirconium ions; Calcium ions; NiO dielectric constant; dielectric loss.

1. Introduction

Perovskite structures such as PbZrTiO_3 (PZT) and $\text{PbMg}_{1/3}\text{Nb}_{2/3}\text{O}_3$ (PMN), exhibit high dielectric constant but both materials have high dielectric loss and also poor temperature stability (Bencan et al., 2012). Besides, they contain lead which is toxic. Most recently, a lead-free perovskite like $\text{CaCu}_3\text{Ti}_4\text{O}_{12}$ (CCTO) has high static dielectric constant at room temperature but its weak temperature is between -173 and 107 °C (Guillemet et al., 2006). The key properties required for a capacitor are high dielectric permittivity and low dielectric loss which can withstand high temperatures. Large dielectric constants of LaMnO_3 and CCTO are interpreted by polarization mechanism from electrically heterogeneous grain and grain boundary regions (Li et al., 2012), but the dielectric loss of the system is

high. However, it is difficult to achieve these two properties simultaneously in a particular material.

In order to achieve these two important properties, high dielectric constant and low dielectric loss in capacitor and memory devices, many materials have been studied and NiO has been found to be one of the promising materials to be used as various applications in supercapacitor, exchange bias controlled spin valve and electrochromic devices and independent with a high temperature. Pure NiO is an insulator at room temperature, nonperovskite, lead free and nonferroelectric (Dutta et al., 2010). The improvement in dielectric properties of NiO becomes very important due to its complex band structure in which the dielectric properties can be tailored by introducing other element into the system. Dakhel, (2012) studied the dielectric properties of NiO at low frequency. Both reports revealed that dielectric constant for pure NiO was 30 and oxygen vacancies were responsible for the dielectric properties of Ni. Several dopants of varying valencies, ionic size and concentrations were added into NiO and the variations in densification, and dielectric properties of NiO were reported.

Thus, this work focuses on the effect doping on the structural and electrical properties of $\text{Ni}_{(1-x)}\text{Zr}_x\text{O}$ and $\text{Ni}_{(1-y)}\text{Ca}_y\text{O}$. Zr^{4+} and Ca^{2+} with atomic radii of 0.079 nm and 0.100 nm, and have the potential to be doped into NiO because they tend to disturb the NiO structure, hence improve the dielectric properties of NiO at room temperature at high frequency range from 1MHz to 1GHz. In this study Zr^{4+} and Ca^{2+} were doped into the NiO system in order to achieve high dielectric constant and low dielectric loss.

2. Experimental

Commercial NiO (Aldrich 99%), Zirconium oxide (ZrO_2), Merck and Calcium oxide (CaO), Merck were used as starting materials. The $\text{Ni}_{(1-x)}\text{Zr}_x\text{O}$, $\text{Ni}_{(1-x)}\text{Ca}_x\text{O}$ and $\text{Ni}_{0.95}\text{Zr}_{0.02}\text{Ca}_{0.01}$ was prepared by using conventional solid state processing technique. Pure NiO was mixed with different amount of Zr^{4+} and Ca^{2+} (0.01, 0.02, 0.03, 0.05 and 0.10) mole%. The starting material of NiO was doped with Zr^{4+} and Ca^{2+} . The composition of Zr^{4+} and Ca^{2+} varied from 0.01, 0.02, 0.03, 0.05 to 0.1 mol%. The raw materials were wet mixed with acetone for 24 hours using zirconia ball as the mixing medium. Then the mixtures were calcined. The calcined powder was then compacted at 250 MPa into 6 and 13 mm diameter pellet shapes by using hydraulic pressing. Sintering process was done at 1280°C for 10 hours using Electrical Carbolite Furnace CWF 1400 with a heating rate and cooling rate of 5°C/min. Table 2.1 and 2.2 shows the parameters involved for $\text{Ni}_{(1-x)}\text{Zr}_x\text{O}$, $\text{Ni}_{(1-x)}\text{Ca}_x\text{O}$ and for $\text{Ni}_{(1-x-y)}\text{Zr}_x\text{Ca}_y$. Characterization and analysis of the samples were carried out by using XRD (BRUKER AXS D8 Diffractometer) for structural analysis and dielectric measurement with Impedance Analyzer (RF Impedance/Material Analyzer 4291B Hewlett Packard).

3. Result and Discussion

3.1 Characterization of sintered $\text{Ni}_{(1-x)}\text{Zr}_x\text{O}$.

(a) X-ray Diffraction Results

Fig.1.(a) shows the XRD result for $\text{Ni}_{(1-x)}\text{Zr}_x\text{O}$ ceramics samples with different Zr^{4+} concentration. Results indicated that there were five peaks similar to the standard pattern of NiO with Miller index (hkl) of (111), (200), (220), (311), and (222). These Miller index were identified as cubic NiO. The peak intensity was getting lower as the concentration of Zr^{4+} increase.

Fig.1(b) shows peaks of $\text{Ni}_{(1-x)}\text{Zr}_x\text{O}$ which corresponded to the (200). The highest $\text{Ni}_{(1-x)}\text{Zr}_x\text{O}$ intensity peak (200) was chosen for the determination of lattice parameter by using the least square refinement method. The incorporation of Zr^{4+} into NiO crystallite led to changes in lattice parameter and crystallite size. There was an increase in the lattice parameter and crystallite size with increased Zr^{4+} contents. Thongbai et al. (2009) also reported the same trend in their work on dielectric relaxation and dielectric response mechanism in (Li, Ti)-doped NiO ceramics. This behaviour was attributed to the fact that Zr^{4+} had bigger ionic radius (0.7Å) as compared to Ni^{2+} which had an ionic radius of (0.69Å) (Dakhel, 2009). The trend was to be linear with more addition of Zr^{4+} . The shifted peak on XRD result showed that Zr^{4+} tended to interstitial the parental atom of crystal structure lattice

structure. Moreover, doping Zr^{4+} into NiO induced a non-uniform strain that caused the lattice plane spacing change and diffraction peak to shift to a new 2 theta position. The changes of lattice parameter at sintering due to crystallite size increased with the increasing temperature and the lattice parameter decreased. Higher amount of Zr^{4+} increased the lattice parameter. So, there was a possibility that Zr^{4+} dopant could alter the structure by changing the lattice parameter of parental host with increasing doping concentrations.

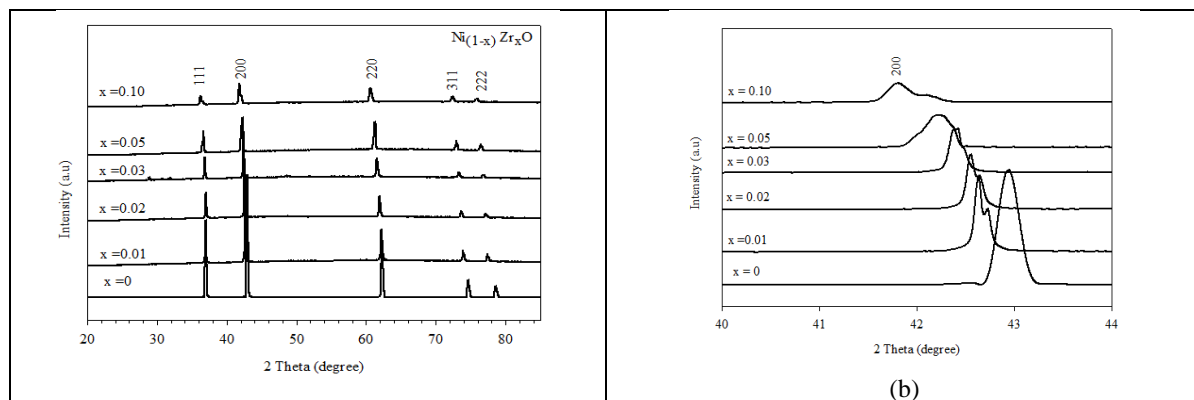


Fig.1: (a) XRD pattern of $\text{Ni}_{(1-x)}\text{Zr}_x\text{O}$ sintered at 1280°C for 10 hours, (b) Close-up of XRD pattern of $\text{Ni}_{(1-x)}\text{Zr}_x\text{O}$ pellet sintered at 1280°C for 10 hours.

(b) Dielectric Behaviour of sintered $\text{Ni}_{(1-x)}\text{Zr}_x\text{O}$

Fig.2. shows frequency dependence of ϵ_r of $\text{Ni}_{(1-x)}\text{Zr}_x\text{O}$ samples as a function of Zr^{4+} doping concentration. It was observed that the ϵ_r decreased with the increasing of frequencies. A rapid decrease of ϵ_r values took place at the frequency range between 1-10 MHz and it became almost linear between 10 MHz-1 GHz.

The ϵ_r of NiO was improved with the addition of Zr^{4+} doping. The Zr^{4+} -doped samples with doping concentrations, $x = 0.01, 0.05$ and 0.10 mole % Zr^{4+} exhibited higher ϵ_r than the undoped NiO sample at frequencies ranging from 1 MHz to 5 MHz. It was apparent that the $x = 0.02$ sample exhibited highest ϵ_r which was 700 at 1 MHz. At 1 MHz, the other sample $x = 0.01, 0.03$ and 0.05 mole % Zr^{4+} exhibited 300, 400 and 200 while the 0.10 % mole Zr^{4+} sample had ϵ_r of 180. The larger at grain size of $x = 0.02$ sample might have contributed to the increase of high dielectric constant. Therefore Zr^{4+} dopant especially at $x = 0.02$ can be used to improve dielectric constant of NiO.

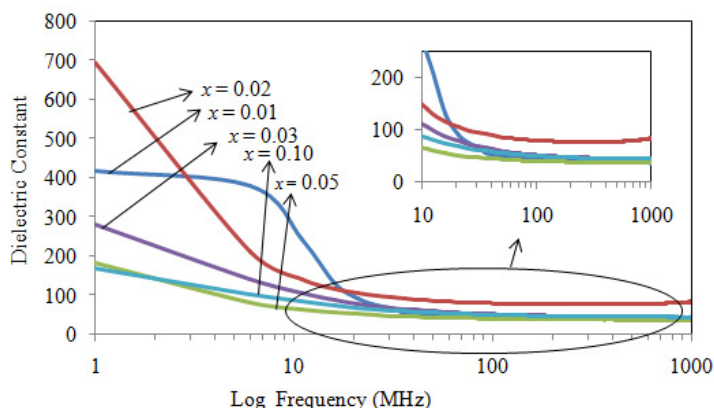


Fig.2. : Frequency dependence of dielectric constant of $\text{Ni}_{(1-x)}\text{Zr}_x\text{O}$ samples as a function of Zr^{4+} doping concentrations.

3.2 Characterization of sintered $\text{Ni}_{(1-x)}\text{Ca}_x\text{O}$

(a) X-Ray Diffraction Result

Fig.3.(a) shows the result for $\text{Ni}_{(1-x)}\text{Ca}_x\text{O}$ ceramic sample with different Ca^{2+} concentration. As seen, the XRD pattern of the entire sintered $\text{Ni}_{(1-x)}\text{Ca}_x\text{O}$ are very similar. Results indicated that there were five peaks similar to the standard pattern of NiO with Miller index of (111), (200), (220), (311) and (222). No other secondary phase formation was detected. There were no obvious changes in peak intensity as the amount of Ca^{2+} increases.

Fig.3.(b) shows peaks of $\text{Ni}_{(1-x)}\text{Ca}_x\text{O}$ which correspond to the (200). The highest $\text{Ni}_{(1-x)}\text{Ca}_x\text{O}$ intensity peak (200) was chosen for the determination of lattice parameter by using the least square refinement method (Appendix H) while crystallite size was calculated by using Debye Scherer equation (Appendix I). The peak was shifted to the smaller angle with the addition of Ca^{2+} contents. The incorporation of Ca^{2+} into NiO led to a change of its lattice parameter and crystallite size. There was an increase in the lattice parameter and crystallite size with increasing amount of Ca contents. The band structure of NiO changed because of Ca doping causes conduction and valance band overlapped in the Fermi level.

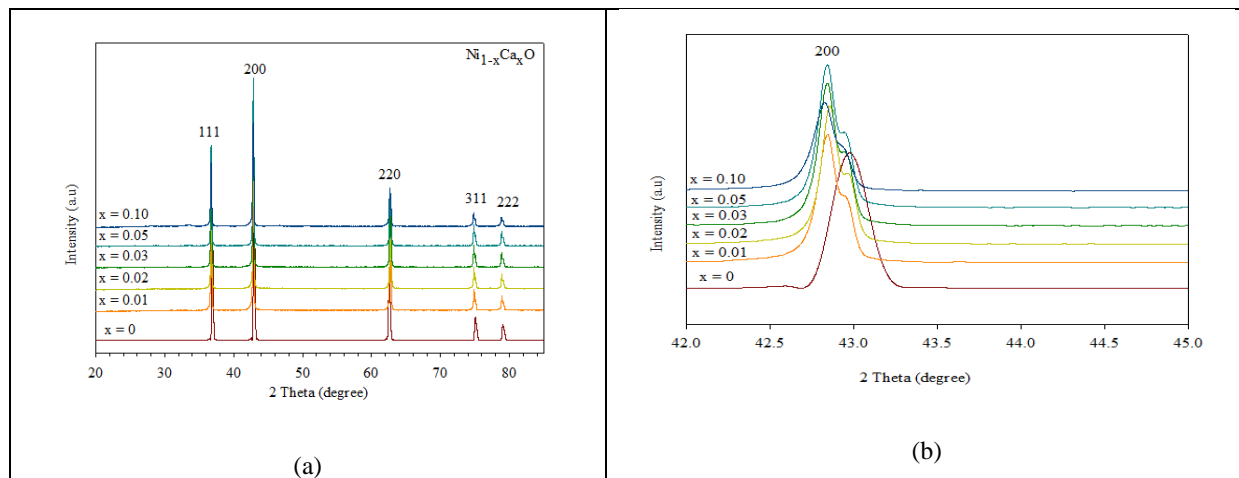


Fig.3. : (a) XRD pattern of $\text{Ni}_{(1-x)}\text{Ca}_x\text{O}$ sintered at 1250°C for 4 hours, (b) Close-up of XRD pattern of $\text{Ni}_{(1-x)}\text{Ca}_x\text{O}$ pellet sintered at 1250°C for 4 hours.

(b) Dielectric Behaviour of Sintered $\text{Ni}_{(1-x)}\text{Ca}_x\text{O}$

Fig.4. shows frequency dependence of ϵ_r for $\text{Ni}_{(1-x)}\text{Ca}_x\text{O}$ samples as a function of Ca^{2+} doping concentration. It was observed that the ϵ_r decreased with the increase of frequencies. The ϵ_r of NiO was improved with the addition of Ca^{2+} doping. The Ca^{2+} -doped exhibited higher ϵ_r than the undoped NiO sample at frequencies range 1 MHz to 5 MHz. It was apparent that the $x = 0.01$ sample exhibited highest ϵ_r which was 123 at 1 MHz. At 1 MHz, the other sample $x = 0.02, 0.03, 0.05$ and 0.10 mole % Ca^{2+} exhibited 120, 115, 102 and 89. The ϵ_r rapidly dropped in the frequency range of 1-10 MHz. It could be explained by the mechanisms of polarization that had varying time response capabilities to an applied field frequency, and polarization contributed to the ϵ_r . A dipole could not keep shifting orientation direction when the frequency of the applied electric field exceeded its relaxation frequency. The relaxation frequency was the reciprocal of the minimum reorientation time for an electric dipole within the alternating electric field⁵.

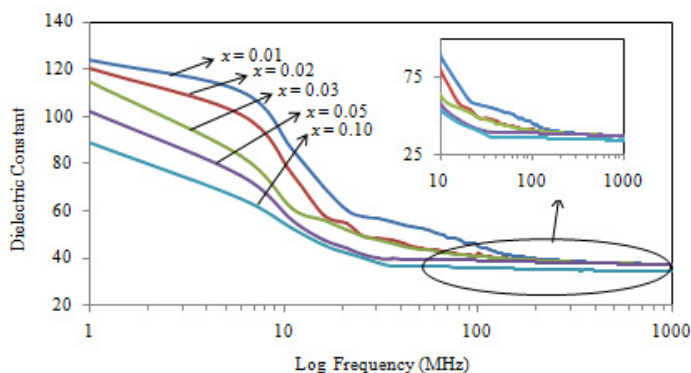


Fig.4. : Frequency dependence of dielectric constant of $\text{Ni}_{(1-x)}\text{Ca}_x\text{O}$ for several mole % of Ca^{2+} .

4. Conclusion

Undoped NiO and Zr^{4+} and Ca^{2+} doped NiO have been successfully prepared by using solid state reaction technique. The presence of $\text{Ni}_{(1-x)}\text{Zr}_x\text{O}$ and $\text{Ni}_{(1-x)}\text{Ca}_x\text{O}$ single phase was obtained by X-ray diffraction for all of the sintered sample. The dielectric behavior of $\text{Ni}_{(1-x)}\text{Zr}_x\text{O}$ with $x = 0.02$ mole % Zr^{4+} exhibited the highest dielectric constant (700) and the lowest dielectric loss value (0.16). The dielectric behavior of $\text{Ni}_{(1-x)}\text{Ca}_x\text{O}$ samples showed that the sample doped with $x = 0.01$ mole % Ca^{2+} obtained the highest dielectric constant (123) and the lowest dielectric loss value (0.05) measured at 1 MHz.

Acknowledgement

The author was very grateful to Universiti Sains Malaysia to support this research, under grant Fundamental Research Grant Scheme (FRGS) – 6730071, and RUI (814184).

References

1. Bencan, A., Mall, B., Drnovsek, S., Tellier, J., Rojac, T., Pavlic, J., Kosec, M., Webber, K. G., Rodel, J. & Damjanovic, D. (2012). Structure and the electrical properties of Pb (Zr, Ti)O₃ zirconia composite. *Journal of the American Ceramic Society*, 95, p. 651-657
2. Guillemet, F, S., Lebey, T., Boulus, M. & Durand, B. (2006). Dielectric properties of CaCu₃Ti₄O₁₂ based multiphase ceramics. *Journal of European Ceramic Society*, 26, p. 1245-1257
3. Li, Y., Fang, L., Liu, L., Huang, Y. & Hu, C. (2012). Giant dielectric response and charge compensation of Li and Co-doped NiO ceramics. *Materials Science and Engineering*, 177, p. 673-677.
4. Dutta, T., Gupta, P., Gupta, A. & Narayan, J.(2010). Effect of Li doping in NiO thin films on its transparent and conducting properties and its application in heteroepitaxial p-n junctions. *Journal of Applied Physics*, 108, p. 083175(1-7).
5. Dakhel, A. (2012). Dielectric relaxation behavior of Li and La co-doped NiO ceramic. *Ceramic international*, 4, p. 4263-4268.